

**SAND20XX-XXXXR**

**LDRD PROJECT NUMBER:** 181202

**LDRD PROJECT TITLE:** Development and Testing of Protection Scheme for Renewable-Rich Distribution System

**PROJECT TEAM MEMBERS:** Sukumar Brahma, Satish Ranade, Mohamed E. Elkhatib, Abraham Ellis, Matthew J. Reno

## **ABSTRACT:**

As the penetration of renewables increases in the distribution systems, and microgrids are conceived with high penetration of such generation that connects through inverters, fault location and protection of microgrids needs consideration. This report proposes averaged models that help simulate fault scenarios in renewable-rich microgrids, models for locating faults in such microgrids, and comments on the protection models that may be considered for microgrids. Simulation studies are reported to justify the models.

## **SECTION I: INTRODUCTION:**

As the penetration of renewables increases in distribution systems, it is significantly impacting protection of such systems. Such generation, that includes photovoltaic (PV), wind, electric vehicle (EV), battery storage, and such, connect through inverters. Inverters are designed to restrict their output current to a low value - typically 110% to 150% of the rated current. Since they can restrict the current quickly (within a cycle), conventional protection, which is based on a combination of overcurrent and undervoltage principles may be inadequate to detect a fault. To complicate the matter further the inverters respond similarly to curtail charging currents of capacitors, transformer inrush, and sudden changes of large inductive loads, including starting current drawn by induction motors.

This project built on the work done by New Mexico State University during the year 2016. During 2016, a current-limited voltage source inverter model was created in time-domain to be used for protection and fault location studies to be performed on microgrids with high penetration of renewable generation interfaced. The model was used to evaluate traditional (overcurrent, undervoltage, sequence components) and new (time-frequency resolution of voltage and current waveform) fault-detection (not location) strategies at the point of interconnection (POI) of the inverter. This work has been published in [1].

The main objective of the 2017 project was to create a model for fault location. Since the inverter is current-limited, and the fault contribution is limited to values similar to load currents, it is of interest if the linear model for short circuit analysis that is used in most fault location methods [2] holds in presence of inverter-interfaced renewables (IIR). The model used for sources in [2] is the Thevenin equivalent, which is shown to work well for synchronous generators assumed as

distributed resources in the paper. However, the inverter output is not only current-limited, but in case of low voltage ride through (LVRT), adjusts its power factor based on the positive-sequence voltage observed at its POI. The behavior is more like a voltage controlled current source, which is essentially nonlinear at the instant of inception of fault, but can be seen as piecewise linear for extended time-frames after the inverter-controls make their impact. This time is typically one to two cycles based on the studies in [1].

This report describes the development of a reduced (averaged) model for the IIRs, and documents results from applying this model to fault-location on microgrid systems that are connected to the grid. The fault-location formulation is tested in positive sequence frame for proof of concept, but can be extended to unbalanced systems.

Next, the averaged model is used to develop a protection model for microgrid with substantial penetration of IIRs. Since the fault current contribution from IIRs are severely limited, it is of interest to evaluate the protection strategy for such systems.

## SECTION II: DETAILED DESCRIPTION OF EXPERIMENT/METHOD:

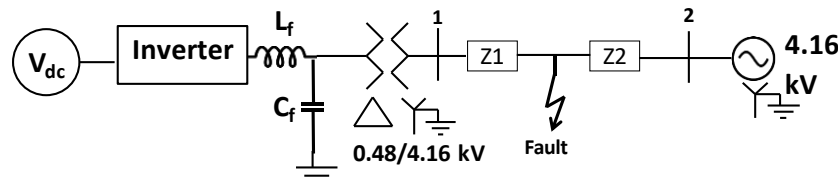


**Figure 1. Inverter interfaced renewable connected to an infinite bus**

The 100 kW inverter modeled in [1], interfaced through a step up transformer is first connected to an infinite bus through a short line modeled as coupled impedances. Voltages and currents before and after the fault are measured at all buses and converted to phasors. The bus impedance matrix is formed treating the whole inverter and transformer as an ideal current source. Thus, the bus impedance matrix is formed *only* with  $Z_1$ ,  $Z_2$ , and the impedance of the infinite source; the transformer and filter impedances are *not* included. There is a  $65+j40$  kVAR load connected to bus 3 (the faulted bus), which is also included in the bus impedance matrix. This is traditional practice with fault analysis because the constant power loads behave as constant impedance loads at low voltages imposed on the system during faults. The fault location model used is linear, which is described in [2], and is based on (1).

For faulted condition, the change in the three-phase voltages at bus  $I$  due to a fault at bus  $J$  is given by (1) for the three-phase model of the system.

$$\Delta V^{(abc)}_{I-J} = Z_{bus}^{(abc)}(I, J) \times I^{(abc)}_F \quad (1)$$

The superscript  $(abc)$  in (1) denotes the three-phase equivalents of the respective elements.  $I^{(abc)}_F$  is the three-phase fault current *injection* at bus  $J$ .  $\Delta V^{(abc)}_{I-J}$  denotes the change in the three-phase voltage values at bus  $I$  due to the injected current  $I^{(abc)}_F$  at bus  $J$ .

To verify if the assumed “ideal current-source” source model fits into the linear fault analysis, various types of balanced and unbalanced faults are created. Fault point is modeled as the third bus, and the positive sequence fault current is measured for each type of fault after two cycles, and converted to phasors. For this value of fault current, change in voltages at each bus is calculated using (1), and compared with the observed voltage changes. Low errors would indicate that the model is valid. Results are documented in section II, and discussion in section III.

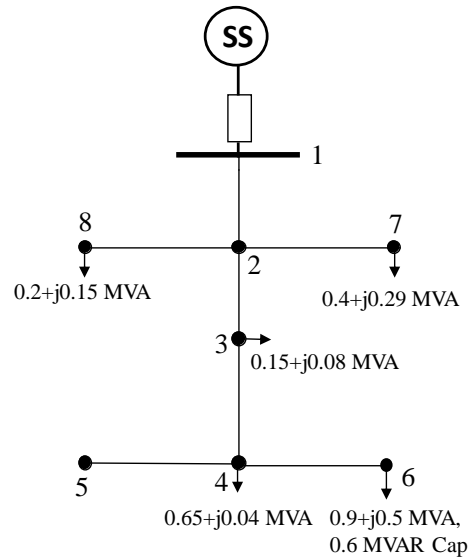


**Figure 2. Test distribution system with 200 kW power injected at buses 4 and 5.**

In order to test the models on a larger network with higher penetration of IIRs, first a voltage controlled ideal current source is created in PSCAD. The model is created with LVRT capability, and the results are documented in the next section. It can be clearly seen from results that the model injects rated power at unity power factor during healthy operation, but increases the reactive power during faults, thus operating in leading power-factor mode, still keeping the magnitude of current below the maximum threshold of 1.1 per unit of rated current. The system selected for testing is an 8-bus distribution system shown in Figure 2. This system is derived from the IEEE 13-bus distribution system [3]. For proof of concept, the system is kept balanced. Two 100 MW voltage controlled current sources are connected to buses 4 and 5 each, through delta/YG transformers, and different types of faults are created on bus 3. The testing method is the same as employed for the smaller (infinite bus) system of Figure 1.

In order for the fault location method based on the linear model to be accurate, the total fault current has to be known as illustrated by equation (1). There are two approaches to find this current, first, when fault current is significantly large compared to load currents, the fault current can simply be calculated as summation of all source currents, which are assumed to be measured. This method works well when the DERs are synchronous generators, as illustrated by [2]. However, in case of IIRs, the fault current is likely to be almost the same as load currents, so this method may give errors. In view of this fact, another method is employed which uses the same linear model but *estimates* the fault current using a state estimator formulation. This formulation is described now.

Sandia National Laboratories is a multimission laboratory managed and operated by National Technology and Engineering Solutions of Sandia LLC, a wholly owned subsidiary of Honeywell International Inc. for the U.S. Department of Energy's National Nuclear Security Administration under contract DE-NA0003525.

For the sake of proof of concept, the fault location method is outlined assuming a balanced system, but can be extended to unbalanced systems. In this case, only the positive sequence component of voltage drop is utilized in the formulation, regardless of the type of fault (3-ph, 2-ph, and 1-ph, with or without ground). Hence, the positive sequence voltage drop at bus  $i$  is (based on (1)):

$$\Delta V_i^{(1)} = -Z_1(i, f) \times I_F^{(1)} \quad (2)$$

where  $I_F^{(1)}$  corresponds to the positive sequence total fault current and  $Z_1(i, f)$  the respective entry of the positive sequence bus impedance matrix.

The fault location can be written as an estimation problem of the following column vector:

$$x(3 \times 1) = \begin{pmatrix} |I_F^{(1)}| \\ \delta_F^{(1)} \\ fl \end{pmatrix} \quad (3)$$

where  $|I_F^{(1)}|$  is the magnitude of the positive sequence total fault current,  $\delta_F^{(1)}$  its respective angle, and  $fl$  the fault location within the faulted line. The estimation of the  $3$  by  $1$  vector in (3) is feasible given 3 linearly independent voltage phasor drop measurements are available. Each  $\Delta V_i^{(1)}$  measurement can be decomposed into its real and imaginary part as in (4):

$$\Delta V_i^{(1)} \rightarrow \begin{cases} \text{Re} [\Delta V_i^{(1)}] \\ \text{Im} [\Delta V_i^{(1)}] \end{cases} \quad (4)$$

By employing the voltage phasor drop measurements at any 3 buses say,  $i=$ "1", "2", and "3", a  $6 \times 3$  Jacobian matrix can be formulated with respect to (3). In our case, we assume synchronized measurements are available at all source buses; only three would suffice.

$$J(6 \times 3) = \begin{pmatrix} \frac{\partial \text{Re} [\Delta V_1^{(1)}]}{\partial |I_F^{(1)}|} & \frac{\partial \text{Re} [\Delta V_1^{(1)}]}{\partial \delta_F^{(1)}} & \frac{\partial \text{Re} [\Delta V_1^{(1)}]}{\partial fl} \\ \frac{\partial \text{Re} [\Delta V_2^{(1)}]}{\partial |I_F^{(1)}|} & \frac{\partial \text{Re} [\Delta V_2^{(1)}]}{\partial \delta_F^{(1)}} & \frac{\partial \text{Re} [\Delta V_2^{(1)}]}{\partial fl} \\ \frac{\partial \text{Re} [\Delta V_3^{(1)}]}{\partial |I_F^{(1)}|} & \frac{\partial \text{Re} [\Delta V_3^{(1)}]}{\partial \delta_F^{(1)}} & \frac{\partial \text{Re} [\Delta V_3^{(1)}]}{\partial fl} \\ \frac{\partial \text{Im} [\Delta V_1^{(1)}]}{\partial |I_F^{(1)}|} & \frac{\partial \text{Im} [\Delta V_1^{(1)}]}{\partial \delta_F^{(1)}} & \frac{\partial \text{Im} [\Delta V_1^{(1)}]}{\partial fl} \\ \frac{\partial \text{Im} [\Delta V_2^{(1)}]}{\partial |I_F^{(1)}|} & \frac{\partial \text{Im} [\Delta V_2^{(1)}]}{\partial \delta_F^{(1)}} & \frac{\partial \text{Im} [\Delta V_2^{(1)}]}{\partial fl} \\ \frac{\partial \text{Im} [\Delta V_3^{(1)}]}{\partial |I_F^{(1)}|} & \frac{\partial \text{Im} [\Delta V_3^{(1)}]}{\partial \delta_F^{(1)}} & \frac{\partial \text{Im} [\Delta V_3^{(1)}]}{\partial fl} \end{pmatrix} \quad (5)$$

A state estimator can now be formed; least error squared (LES) or least absolute value (LAV) being a couple of choices. An initial guess in (3) can be made equal to the summation of all source currents, and fault location  $fl$  can be assumed initially to be 0.5, meaning the assumed fault location

is in the middle of line. Based on the real and imaginary parts of the voltage phasor drop measurements, the measurement vectors can be written as in (6) and (7).

$$z_{\text{Re}} = \begin{pmatrix} \text{Re} \left[ \Delta V_1^{(1)} \right] \\ \text{Re} \left[ \Delta V_2^{(1)} \right] \\ \text{Re} \left[ \Delta V_3^{(1)} \right] \end{pmatrix} \quad (6)$$

$$z_{\text{Im}} = \begin{pmatrix} \text{Im} \left[ \Delta V_1^{(1)} \right] \\ \text{Im} \left[ \Delta V_2^{(1)} \right] \\ \text{Im} \left[ \Delta V_3^{(1)} \right] \end{pmatrix} \quad (7)$$

Using the current value of (3), the respective measurement functions and the measurement mismatches are updated based on (8) – (10).

$$h_{\text{Re}}(x) = \begin{pmatrix} \text{Re} \left[ -Z_1(1, f) \times I_F^{(1)} \right] \\ \text{Re} \left[ -Z_1(2, f) \times I_F^{(1)} \right] \\ \text{Re} \left[ -Z_1(3, f) \times I_F^{(1)} \right] \end{pmatrix} \quad (8)$$

$$h_{\text{Im}}(x) = \begin{pmatrix} \text{Im} \left[ -Z_1(1, f) \times I_F^{(1)} \right] \\ \text{Im} \left[ -Z_1(2, f) \times I_F^{(1)} \right] \\ \text{Im} \left[ -Z_1(3, f) \times I_F^{(1)} \right] \end{pmatrix} \quad (9)$$

$$\Delta z = \begin{pmatrix} z_{\text{Re}} - h_{\text{Re}}(x) \\ z_{\text{Im}} - h_{\text{Im}}(x) \end{pmatrix} \quad (10)$$

Eventually, a linear programming (LP) problem is formulated as shown in (11), and it is solved for each iteration. The Jacobian matrix (5) is updated for every iteration.

$$\begin{array}{ll} \min & c'y \\ \text{s.t.} & Ay = \Delta z \end{array} \quad (11)$$

The estimation vector is updated according to (12) and (13).

$$\Delta x = \begin{pmatrix} y(1) - y(4) \\ y(2) - y(5) \\ y(3) - y(6) \end{pmatrix} \quad (12)$$

$$x_{\text{new}} = x_{\text{old}} + \Delta x \quad (13)$$

The termination strategy is defined in (14). The final solution of vector  $x$  gives the fault location, since element  $x(3)$  corresponds to  $fl$ .

Finally, conventional protection models are evaluated on the 8-bus system. Comments and observations are documented in sections III and IV.

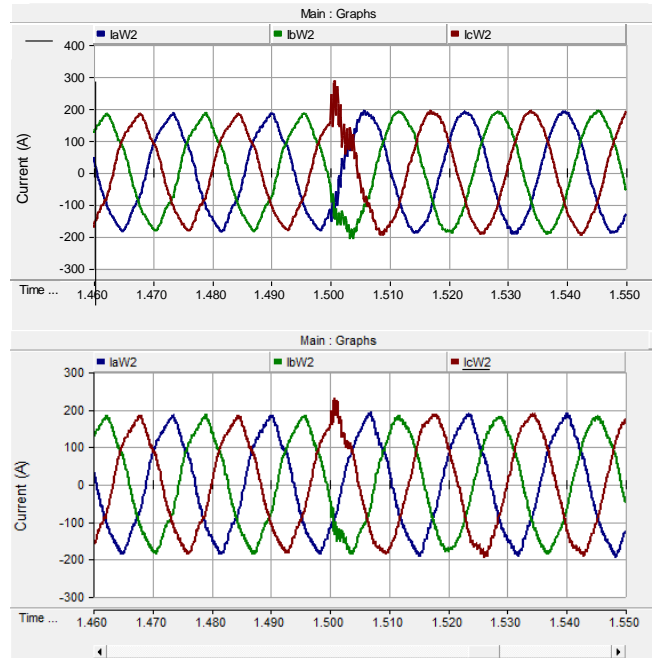


**Figure 3. Inverter output for a) 3-ph fault and b) Phase B-G fault on bus 3 in the system shown in Figure 1.**

## SECTION III: RESULTS:

### Inverter Performance and Fault Location Results for the System in Figure 1:

Figure 3 (a) and (b) show the inverter output for a three-phase and a line-to ground fault, respectively, on bus 3 at 1.5 s. into the simulation. Observe the current limited output under faulted conditions. Four types of faults with nominal fault-resistance values were created on bus 3 and the errors between calculated and observed voltage changes at all three buses were noted using the injected current as *option 1*: sum of both source currents, and *option 2*: the observed fault current in the simulation. These are tabulated in Table 1.

**Table 1. Errors in Fault Location for the system in Figure 1.**

Type of Fault	%Error in $ \Delta V_1 $		%Error in $ \Delta V_2 $		%Error in $ \Delta V_3 $	
	<i>option 1</i>	<i>option 2</i>	<i>option 1</i>	<i>option 2</i>	<i>option 1</i>	<i>option 2</i>
3-ph	0.43	0.31	0.43	0.58	0.71	0.58
L-G	5.83	1.64	5.21	1.04	5.21	1.04
L-L-G	2.36	1.04	3.04	1.71	3.04	1.71
L-L	2.01	0.43	2.23	0.62	2.18	0.62

There is some indication from the results that the low fault contribution from the inverter does introduce larger errors, and the state estimator based method would provide better accuracy. This also validates the constant current source model for the inverter.



## Results Illustrating the Voltage Controlled Current Source Model with LVRT:

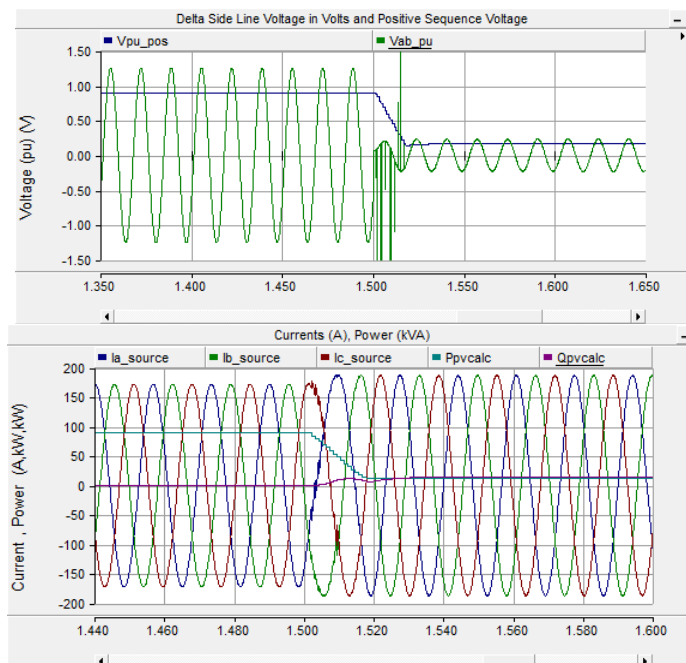


**Figure 4. a) Voltage output and b) current and power output of the voltage controlled current source for a 3-ph fault on bus 3 in the system shown in Figure 1.**

The inverter in the system in Figure 1 is replaced by a voltage controlled current source modeled in PSCAD to replicate the inverter behavior. The LVRT conditions are imposed through a table with 10 discrete values. Figure 4 (a) shows the voltage output (including positive sequence voltage used to impose LVRT conditions), and Figure 4 (b) shows current and power output of the source model for a three-phase fault. Figure 5 shows these quantities for a line-to-ground fault. Clearly the results model the inverter behavior accurately in healthy and faulted conditions, plus it changes the reactive power input during fault, thus modeling LVRT.

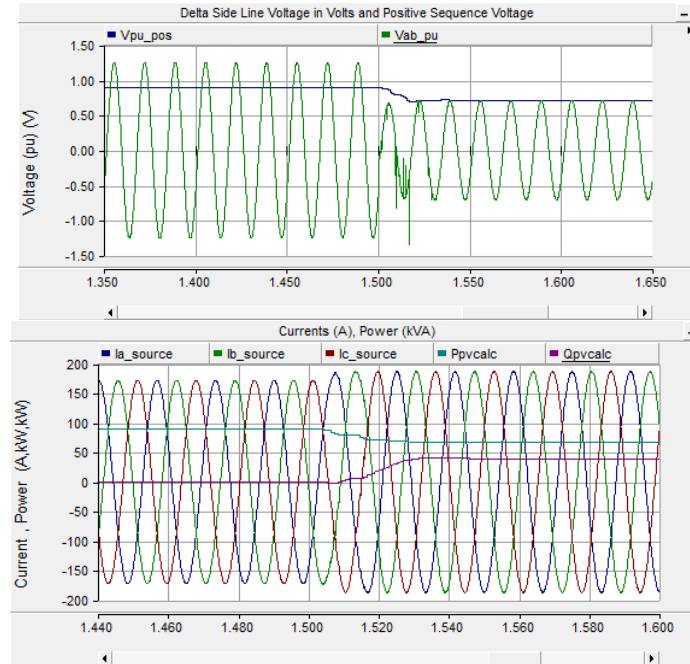


**Figure 5. a) Voltage output and b) current and power output of the voltage controlled current source for a L-G fault on bus 3 in the system shown in Figure 1.**

#### Fault Location Results for the System in Figure 2:

For different types of faults at bus 3, the errors in voltage changes observed and calculated at all 8 buses are documented in Table 2 using the injected current as *option 1*: sum of both source currents, and *option 2*: the observed fault current in the simulation.

**Table 2. Errors in Fault Location for the system in Figure 2.**

%Errors→	ΔV <sub>1</sub>		ΔV <sub>2</sub>		ΔV <sub>3</sub>		ΔV <sub>4</sub>		ΔV <sub>5</sub>		ΔV <sub>6</sub>		ΔV <sub>7</sub>		ΔV <sub>8</sub>	
	Options		Options		Options		Options		Options		Options		Options		Options	
Fault	1	2	1	2	1	2	1	2	1	2	1	2	1	2	1	2
3-ph	3.24	1.36	3.24	1.36	3.24	1.36	3.33	1.45	3.41	1.52	3.33	1.45	3.24	1.36	3.24	1.36
L-G	28.16	2.58	28.20	2.61	28.20	2.61	28.42	2.78	28.61	2.94	28.42	2.78	28.19	2.60	28.19	2.58
L-L	12.41	2.59	12.44	2.62	12.44	2.62	12.65	2.81	12.83	2.98	12.65	2.81	12.44	2.62	12.44	2.62
L-L-G	11.77	1.61	11.77	1.61	11.77	1.61	11.90	1.73	12.01	1.83	11.90	1.73	11.77	1.61	11.77	1.61

## SECTION IV: DISCUSSION:

The low values of errors in Table 1 indicates that the inverter can certainly be modeled as an ideal current source. This means the filter components of inverters, and most importantly, impedance of the interfacing transformer does not need to be included in the bus admittance (and impedance) matrix of the systems. This is different than the Thevenin model we associate with most conventional sources.

Waveforms in Figures 4 and 5 show that the voltage controlled current source model emulates the inverter behavior very well. The significance of this observation is that systems with high

Sandia National Laboratories is a multimission laboratory managed and operated by National Technology and Engineering Solutions of Sandia LLC, a wholly owned subsidiary of Honeywell International Inc. for the U.S. Department of Energy's National Nuclear Security Administration under contract DE-NA0003525.



penetrations of IIRs can be simulated and studied for fault analysis and protection purposes without having to use bulky time-domain models of inverters that are computationally intensive and might require extensive tuning of controls for the system to be stable in the first place.

As for fault location methods, the linear model remains relevant, but the approach of calculating total fault current as the summation of all source currents comes under scrutiny. The error with the first option can be huge, especially for unbalanced faults (where not all three phases see a large positive sequence fault contribution from substation source), because the IIRs are current limited and fault current contributed by them is very similar to load current, introducing large errors between the actual fault current and summed source currents. Due to this reason, the state estimation based approach described in section II may be favorable. The approach was tried on the 8-bus system of Figure 2, and the total fault current estimations were very close to the values observed in simulation. It should be remembered that the methods are tried using positive sequence quantities, so even though the fault currents from POI of IIRs are high for ground faults (due to transformer secondary forming a zero-sequence source), the limits imposed on the positive sequence currents by inverters do affect the method the same way as phase faults. It will be extremely interesting to assess the performance of these methods for islanded mode, especially if the island is totally fed through IIRs. This is because fault currents will be seriously impacted by pre-fault (load) currents.

It should be mentioned here that the fault location models can only benefit from any added sensors in the microgrid. For example, if micro-PMUs are available at all buses, determining the actual fault current would become a non-issue, and there would not be any need for state estimation based approach. The purpose of this project is to develop and test models without any restrictive conditions of implementation.

Protecting such systems is a serious compromise between resiliency and cost. On one hand, if the interfacing transformer on the delta side is not grounded, which is not an unusual practice to restrict total ground fault currents (systems are designed for fault currents only from substation), due to restricted phase currents the protection coordination for the originally radial system may not necessarily be disrupted for every topology and every placement of IIR. However, this comes at the cost of resiliency, because no islanding is conceived.

The one of the driving motivations behind smart grid is to provide better resiliency. Therefore, distribution systems must be allowed to island; in other words microgrids must be designed to be viable under grid-connected as well as islanded modes. This criterion was extensively studied for a military microgrid with diesel generators as distributed resources [4]. The main take away from that study is that even with synchronous generators serving as DER, the difference between fault contribution from grid is much larger than the contribution from DER, which results in improper coordination between overcurrent devices in islanded mode, thus rendering directions overcurrent based approach not viable. In the present study, this observation is going to hold, because the phase fault currents from IIRs is even lower. Detection of fault at the IIR-bus was studied in detail in [5] showed the effectiveness of undervoltage based detection for phase faults and zero-sequence based detection for ground faults (imposing grounded Y secondary of the interfacing transformer). Though zero-sequence based method was able to capture all ground faults, undervoltage based

Sandia National Laboratories is a multitechnology laboratory managed and operated by National Technology and Engineering Solutions of Sandia LLC, a wholly owned subsidiary of Honeywell International Inc. for the U.S. Department of Energy's National Nuclear Security Administration under contract DE-NA0003525.

scheme may not be successful for remote phase faults on a large microgrid. These observations will also hold for the present study. Since there will be substantial current difference between contributions from source and contributions from IIRs, the differential scheme suggested and implemented in [4] will work in the grid-connected mode. However, for islanded microgrids fed completely by IIRs, the protection may become tricky, especially for phase faults, since the fault current are seriously affected by load currents. This, along with the fault location problem for such systems, as mentioned earlier, will be the focus of the next LDRD project.

## **SECTION V: ANTICIPATED OUTCOMES AND IMPACTS:**

The 2018 LDRD will focus on investigating protection models for distribution systems with 100% renewable generation, which are envisaged by the US Department of Energy under their Sun Shot initiative [6]. Most renewables connect through inverters, therefore it is of value to study protection of distribution feeders fed completely by inverter-interfaced generation.

Inverter controls will be a necessary component of this research as they drive the response of the system to faults. The inverters can arrest the magnitude of fault currents to low values (comparable with load currents) within one to two cycles. This poses a challenge to protection, especially in the islanded mode, where no traditional strong source of fault current is present and fault currents are dependent on load currents. This is an unprecedented scenario for protection engineers, because traditional short-circuit analysis used for setting relays allows neglecting load currents in comparison with fault currents.

The specific tasks we propose to accomplish are:

- 1) Model a system with multiple inverters connected and controlled to form a stable island. The model will be simulated in time-domain. The model behavior will be emulated by the averaged model developed and reported in this report.
- 2) Record the fault response of such system for faults on different sections of the feeder.
- 3) Evaluate the protection schemes that are traditionally used for detection and location of fault on the faulted section, and explore new models, based on the results.
- 4) Demonstrate the effectiveness of the new models through extensive simulations in both grid-connected and islanded modes. Formulate viable protection and fault location schemes based on the results.
- 5) Create a test-bed that cosimulates power systems and communication platforms to enable real-time testing of the new protection models and schemes.
- 6) DC microgrids are also a fast-evolving area, and we would also like to explore the protection issues for such microgrids. A literature survey of control strategy of dc/dc converters, and their response to faults is therefore proposed. Challenges to protection of such microgrids and published literature on protection of dc microgrids will be studied. Objectives of the next phase of research will be developed based on this study.

## SECTION VI: CONCLUSION:

This report documents an averaged time-domain model to emulate the steady state and fault behavior of inverter-interfaced renewables, proposes a state-estimator based model for fault location in grid-connected microgrids with high penetration of renewables, and discusses the protection models that would work for such systems. Simulation results show that the averaged model faithfully reproduces the behavior of inverter-interfaced renewables, including the low voltage ride through features during faults. The tests on the fault location model show that the linearity assumption is still valid despite the current limited behavior of inverters during fault, but a state estimation based model is recommended to implement the fault location method because of the fault current contributions from inverters being comparable to load currents. If enough sensors are available in the system to measure the actual fault current, then state estimation is not needed. It was found that the protection models investigated for microgrids in previous work with Sandia National Laboratory would still hold for the microgrids under consideration because of the strong substation source being present in both configurations. However, all the reported models need to be revisited in case of islanded operation of microgrids with bulk of the generation coming from renewables. This work has already begun and will form a large part of the next grant.

## REFERENCES:

- [1] Theodoros Alexopoulos, Milan Biswal, Sukumar Brahma, and Mohamed El Khatib, "Detection of Fault using Local Measurements at Inverter Interfaced Distributed Energy Resources," *Proc. IEEE PES PowerTech 2017*, Manchester, UK.
- [2] Sukumar Brahma, "Fault Location in Power Distribution System with Penetration of Distributed Generation", *IEEE Trans. Power Delivery*, vol. 26-3, pp. 1545 - 1553.
- [3] IEEE 13-node distribution system test feeder, IEEE Distribution System Analysis Subcommittee, online. Available: <https://ewh.ieee.org/soc/pes/dsacom/testfeeders/>
- [4] Sukumar Brahma, Jonathan Trejo, and Jason Stamp, "Insight into Microgrid Protection", *Proc. IEEE PES Innovative Smart Grid Technologies Conference, Europe*, Istanbul, October 2014.
- [5] Theodoros Alexopoulos, Milan Biswal, Sukumar Brahma, and Mohamed El Khatib, "Detection of Fault using Local Measurements at Inverter Interfaced Distributed Energy Resources," *Proc. IEEE PES PowerTech 2017*, Manchester, UK.
- [6] US Department of Energy – ENERGISE, online available: <https://eere-exchange.energy.gov/FileContent.aspx?FileID=f813c864-a235-4d49-85e1-73820cb64ac9>